American Mineralogist, Volume 78, pages 1143–1148, 1993

Raman study of the high-pressure behavior of forsterite (Mg_2SiO_4) crystal and glass

DAN J. DURBEN,* PAUL F. MCMILLAN, GEORGE H. WOLF
Chemistry Department, Arizona State University, Tempe, Arizona 85287, U.S.A.

ABSTRACT

The pressure dependence of the vibrational modes of forsterite (Mg_2SiO_4) crystal and glass were measured to 50 GPa at 298 K with Raman spectroscopy. Raman bands of crystalline forsterite persist to 50 GPa. There is no evidence of the metastable olivine structure converting to more stable spinel or spinelloid structures or undergoing pressure-induced amorphization below 50 GPa. Rather, two new Raman bands appear above 30 GPa. On decompression the new bands are retained to 8 GPa. The spectral changes are interpreted as indicating a defective olivine structure in which Si-O-Si linkages are formed between adjacent SiO_4 tetrahedra on compression, as a prelude to amorphization at higher pressures. For forsterite glass, there is an increase in the breadth of the main Raman band above 20 GPa, arising primarily through an increase in intensity on its low-frequency side. The spectra are consistent with a reversible formation of Si-O-Si linkages in the glass at high pressures.

INTRODUCTION

The high-pressure behavior of orthosilicates at geologically relevant pressures has been the focus of much recent experimental and theoretical investigation. In particular, a number of olivine-structured compounds are now known to amorphize when pressurized well beyond their thermodynamic stability fields (Richard and Richet, 1990; Williams et al., 1990; Guyot and Reynard, 1992; Bouhifd et al., 1992). The high-pressure structural changes in metastable crystalline olivines that precipitate this amorphization are presently not well characterized. In addition, little is yet known about the high-pressure behavior of orthosilicate glasses or melts.

The high-pressure transformation of Mg-rich olivines to the more stable spinel or wadsleyite (β-Mg_2SiO_4) phases is kinetically inhibited at temperatures below 500 °C (Sung and Burns, 1976), allowing the olivine structure to be metastably pressurized well beyond its thermodynamic stability boundary. In forsterite, in situ X-ray diffraction (Hazen, 1976; Kudoh and Takéuchi, 1985; Will et al., 1986) and vibrational spectroscopy (Besson et al., 1982; Xu et al., 1983; Hofmeister et al., 1989; Chopelas, 1990; Wang et al., 1993) indicate a decrease in Si-O and Mg-O bond lengths during room-temperature static compression to ~9 GPa. Small kinks observed in the pressure derivatives of some of the Raman bands near 9 GPa have been interpreted as a possible second-order phase transition (Chopelas, 1990) or as a change in compression mechanism (Wang et al., 1993) that may be related to the cessation of Mg-O bond compression in one of the two types of MgO_6 polyhedra found in the ambient structure (Kudoh and Takéuchi, 1985). No other significant structural changes, other than continued bond compression, are evident in the X-ray and vibrational data to 30 GPa.

TEM data on forsterite statically compressed to over 30 GPa and laser heated to moderate temperatures (<700 °C) suggest an increase in disorder of the cation sublattice with increasing pressure and complete amorphization above 70 GPa (Guyot and Reynard, 1992). Lattice dynamics calculations suggest this behavior may be caused by a dynamic instability in the forsterite structure near 30 GPa.

Shock compression data of forsterite suggest that the olivine structure persists to ~50 GPa, where the Hugoniot temperature is estimated to be ~400 °C (Brown et al., 1987). Between 50 and 80 GPa along the Hugoniot, the olivine structure collapses to an assemblage with an extrapolated zero pressure density that is ~20% denser than forsterite (Brown et al., 1987). The room-pressure density of spinel is only ~10% greater than forsterite. The observation of $MgSiO_3$ glass and MgO in forsterite samples recovered from shock pressures in excess of 100 GPa has been used to suggest that olivine decomposes to a perovskite and magnesiowüstite assemblage under dynamic compression (Syono et al., 1981; Syono and Goto, 1982). More recently, however, it has been suggested that the density increase observed along the Hugoniot of olivine, and of other minerals as well, could result from the transition from a crystal to an amorphous material triggered by strain-induced coordination changes in the metastable crystal (Williams et al., 1990; Jeanloz and Kruger, 1992). Natural olivine samples shocked up to 60 GPa show broad features in the Raman spectrum that have been interpreted as arising from an amorphous phase of unknown composition formed under shock compression (Heymann and Cellucci, 1988).

* Present address: College of Applied Science and Technology, Black Hills State University, Spearfish, South Dakota 57799, U.S.A.

0003–004X/93/1112–1143$02.00

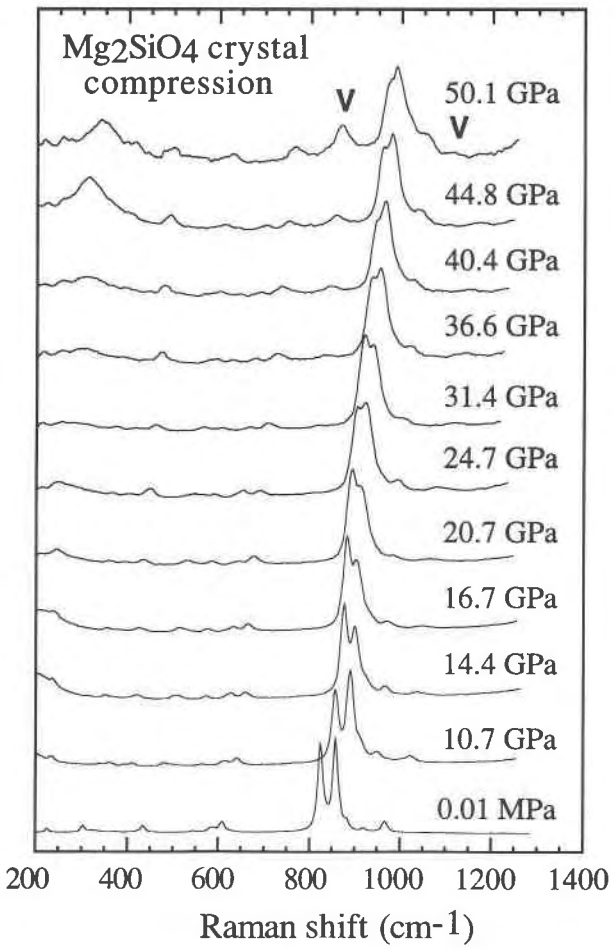

Fig. 1. In situ Raman spectra of crystalline forsterite under compression. Arrows mark new bands that appear above ~30 GPa. Spectral changes near 300 cm^{-1} are obscured by a broad band due to the Ar pressure medium.

To gain further insight into the metastability limits of Mg-rich olivines and their pressure-induced structural transformations under kinetically hindered conditions, we have investigated the high-pressure behavior of both crystalline and amorphous forsterite (Mg_2SiO_4) with in situ Raman spectroscopy at room temperature. We have extended the vibrational spectroscopic data of crystalline forsterite to higher pressures than previous studies and have obtained some of the first high-pressure Raman spectroscopic data of an orthosilicate glass.

Experimental

Forsterite glass was prepared by splat quenching the melt (Williams et al., 1989). Forsterite crystals were selected from crystallized portions of the glass sample and appeared polycrystalline under crossed polars. Samples were loaded into a Mao-Bell type diamond-anvil cell along with condensed Ar as a pressure medium. Pressure was determined by the calibrated shift of the R_1 ruby fluorescence band (Mao et al., 1986). The ruby fluorescence bands remained sharp and distinct even at the highest pressures and indicated a pressure gradient of <5% across the sample. Room-temperature Raman spectra were collected with the micro-Raman system described by Durben and Wolf (1991). The 135° scattering geometry precluded orientational studies of the Raman band intensities at high pressure.

Results and discussion

High-pressure crystal behavior

In situ Raman spectra of crystalline forsterite measured as a function of pressure to 50 GPa are shown in Figure 1. The low-pressure spectra (<30 GPa) and Raman band pressure shifts (Fig. 2) are similar to those reported in previous vibrational studies (Besson et al., 1982; Xu et al., 1983; Hofmeister et al., 1989; Chopelas, 1990; Wang et al., 1993). Although slight kinks are evident in the pressure derivatives of some of the Raman bands near ~9 GPa, no bands are lost and no new bands appear, consistent with the observations of Wang et al. (1993).

The vibrational data at higher pressures indicate that, despite compression to well outside the olivine stability field of forsterite, the relatively sharp Raman bands assigned to vibrations of the olivine crystal structure are retained to 50 GPa. The Raman spectra show no clear evidence for an olivine-to-spinel conversion or pressure-induced amorphization in this pressure range. However, the spectra do indicate that there is some modification of the olivine structure above 30 GPa. Most apparent is the emergence of two new Raman bands above 30 GPa: a relatively strong band near 825 cm^{-1} (with an extrapolated ambient position of ~750 cm^{-1}) and a weaker band near 1060 cm^{-1} (with an extrapolated ambient position of ~960 cm^{-1}). Changes in the low-frequency region are obscured by a large band because of scattering from the Ar pressure medium. The appearance of the new bands is accompanied by a slight kink in the pressure derivative of many of the olivine Raman bands near ~30 GPa (Fig. 2).

The reversibility of these spectral changes was explored by obtaining in situ Raman spectra along the decompression path (Fig. 3). For samples compressed to a peak pressure of 50 GPa, the new high-pressure bands in the Raman spectrum are retained on decompression to ~8 GPa. The increased intensity of the band at 960 cm^{-1}, relative to the band at 750 cm^{-1}, may be an effect of the sample orientation or may indicate that the two bands represent vibrations of different structural units. Below 8 GPa both of the new bands disappear. On recovery of the sample at ambient conditions, the olivine bands return to their initial frequencies.

The changes in the spectra above 30 GPa resemble, at first sight, the typical behavior observed for a second-order phase transition in which a lowering of symmetry allows new bands to become Raman active and produces kinks in the pressure derivatives of the original Raman bands at the transition. However, this explanation is not

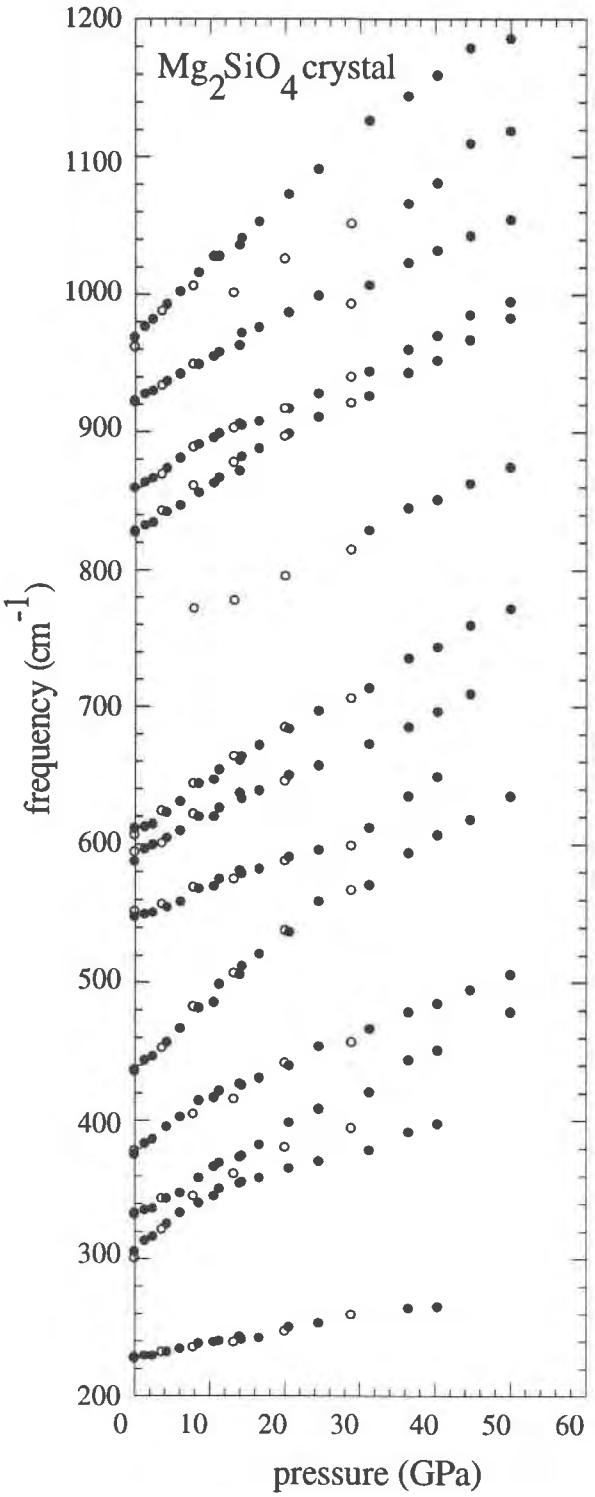

Fig. 2. Pressure dependence of the Raman mode frequencies of crystalline forsterite under compression (solid circles) and decompression (open circles).

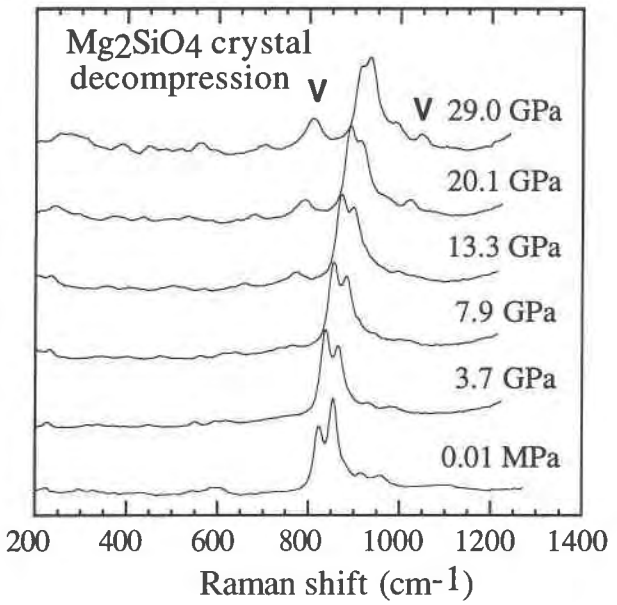

Fig. 3. In situ Raman spectra of crystalline forsterite under decompression. Arrows mark new bands that disappear below ~8 GPa.

likely, since the measured vibrational density of states of forsterite (Rao et al., 1988; Chopelas, 1990) does not reveal any modes in the spectral region in which the most intense new Raman band appears (~750 cm^{-1}). Moreover, the large hysteresis in the emergence and disappearance of the new bands during the cycling of pressure indicates an activation barrier to the structural change responsible for the new bands. A first-order phase change to spinel, modified spinel (β-phase), or other spinelloid phases can be ruled out, since these more stable phases are not recovered upon decompression. In addition, the frequencies of the new bands do not correspond to any other known orthosilicate structure.

More plausible than a periodic structural rearrangement is that the spectral changes represent a build-up of defects in the metastable olivine structure above 30 GPa. The spectral data are consistent with the interpretation that high-pressure defects are formed by polymerization of adjacent SiO_4 tetrahedra. The new 750-cm^{-1} band occurs in a frequency range typical of symmetric stretching vibrations of Si-O-Si dimer linkages, as observed in pyrosilicate structures and β-Mg_2SiO_4 (Piriou and McMillan, 1983; McMillan and Akaogi, 1987). The assignment of the weaker high-frequency band near 960 cm^{-1} is more ambiguous. This band may be caused by asymmetric stretching vibrations of Si-O-Si linkages or vibrations of SiO_3 terminal groups, or it may indicate the formation of higher silicate polymers (Piriou and McMillan, 1983; McMillan and Akaogi, 1987).

Whether these dimer defect species involve tetrahedral or higher coordinate (fivefold or sixfold) Si cannot be unambiguously determined from the Raman data. Maintaining fourfold-coordinated Si during the linkage of two

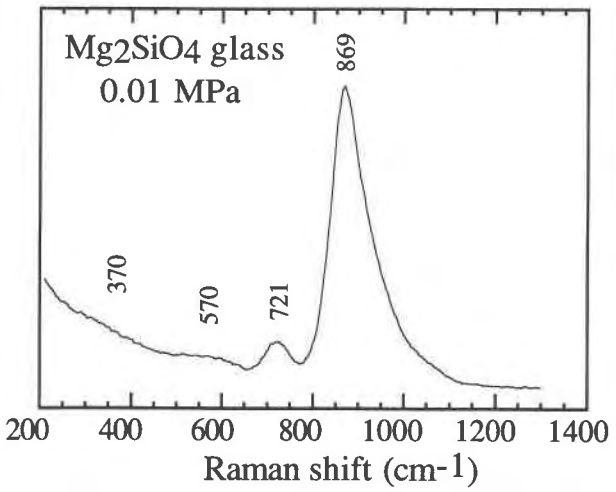

Fig. 4. Ambient Raman spectrum of forsterite glass.

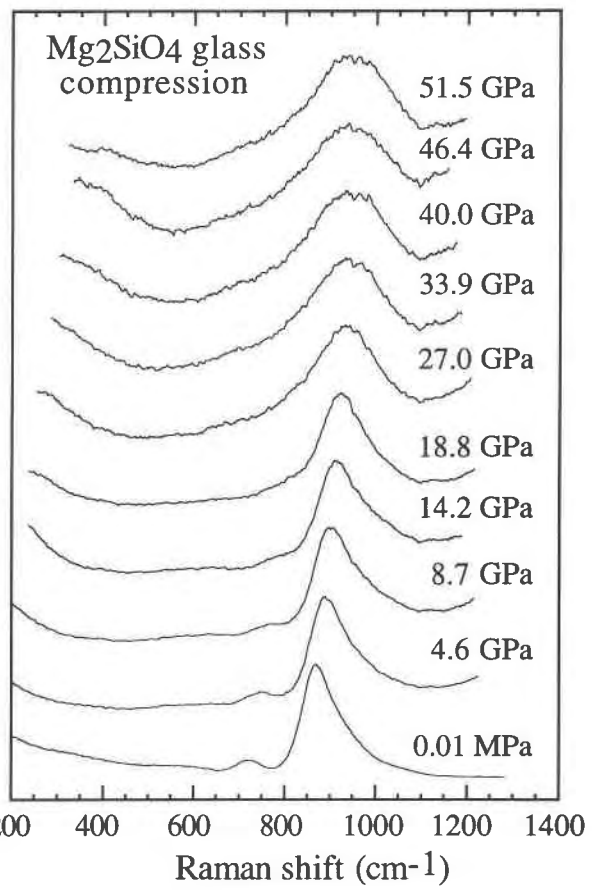

Fig. 5. In situ Raman spectra of forsterite glass under compression. The main Raman band broadens significantly above ~20 GPa, primarily through an increase in intensity between 700 and 900 cm^{-1}.

SiO_4 tetrahedra (to form an Si_2O_7 dimer) would require breaking a Si-O bond, leaving one O atom per dimer only bonded to Mg, as is found in β-Mg_2SiO_4. Formation of an Si_2O_8 dimer would not require Si-O bond breakage but would require a Si coordination change. The assignment of the new 750-cm^{-1} band to vibrations involving high-coordinate Si polyhedral species would then be consistent with the interpretation of Williams et al. (1990) of new IR bands that appear between 600 and 900 cm^{-1} in fayalite above 20 GPa. The assignments of the 750-cm^{-1} band to Si-O-Si linkages or to high-coordinate Si species need not be mutually exclusive: McMillan et al. (1989) have assigned a peak at 602 cm^{-1} in the Raman spectrum of $MgSiO_3$ garnet to a vibration of a $^{[4]}$Si-O-$^{[6]}$Si linkage.

It is interesting to note that there is no appreciable volume change indicated in the Hugoniot until a pressure of about 50 GPa (Brown et al., 1987). At most there is only a slight decrease of the pressure derivative of the bulk modulus above 30 GPa. This would seem to indicate that either the intrinsic local density of the defects is not much greater than that of compressed olivine, or, more likely, that a critical density of defects, sufficient to cause the olivine structure to become amorphous, is not yet achieved under compression up to 50 GPa.

High-pressure behavior of glass

The ambient Raman spectrum of forsterite glass (Fig. 4) is dominated by a broad, asymmetric band with a peak position at 869 cm^{-1}. The principal component of this main Raman band has been assigned to the symmetric stretching vibration (ν_1) of the isolated SiO_4 tetrahedra, with the high-frequency asymmetry arising primarily from the contribution of asymmetric Si-O stretching vibrations (ν_3) (Williams et al., 1989; Cooney and Sharma, 1990). The weak band near 721 cm^{-1} is caused by the bending vibration of a small population of Si_2O_7 dimers in the ambient glass (Williams et al., 1989). Si-O stretching vibrations of these groups also contribute to the high-frequency band profile. Weak bands are also observed near 570 and 370 cm^{-1}, which are most likely caused by ν_2 and ν_4 bending vibrations of the SiO_4 tetrahedra, coupled with Mg-O stretching modes. The overall band profile of the Mg_2SiO_4 glass spectrum is similar to the envelope of peaks in the crystalline forsterite spectrum, suggesting that the ambient short- and intermediate-range structure of the glass is comparable to that of the low-pressure crystalline polymorph.

In situ Raman spectra of forsterite glass to ~50 GPa are shown in Figure 5. The intensity of the spectrum gradually weakens with pressure but is still well resolved at 50 GPa. Under initial compression, the frequency of the main 869-cm^{-1} band increases at a rate of 2.9 cm^{-1}/GPa (Fig. 6), similar in magnitude to the pressure shifts of the strong tetrahedral stretching bands in crystalline forsterite. The weak 721-cm^{-1} band has a positive frequency shift of 4.2 cm^{-1}/GPa, consistent with a tightening of the Si-O-Si angles within the Si_2O_7 species. The intensity of the dimer band decreases with increasing pressure and cannot be followed above ~20 GPa. However, it is difficult to distinguish whether this apparent

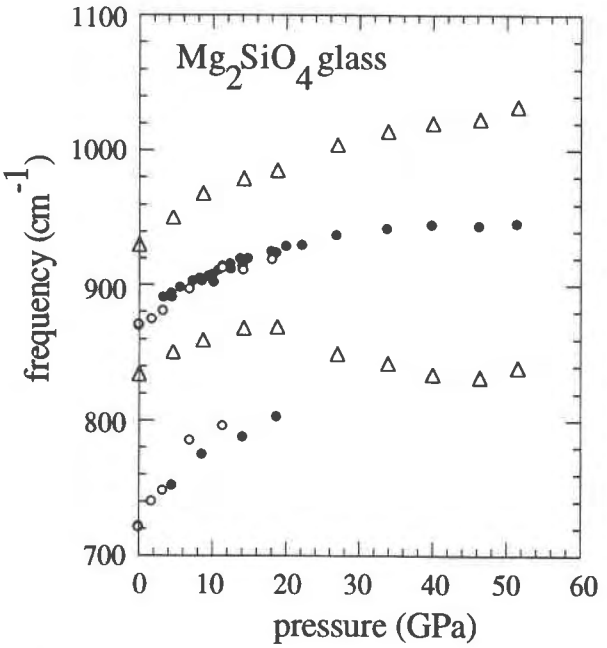

Fig. 6. Pressure dependence of the Raman mode frequencies of forsterite glass under compression (solid circles) and decompression (open circles). Open triangles represent the FWHM frequencies of the main 869-cm^{-1} Raman band on compression and show that most of the broadening of this band above ~20 GPa occurs on its low-frequency side.

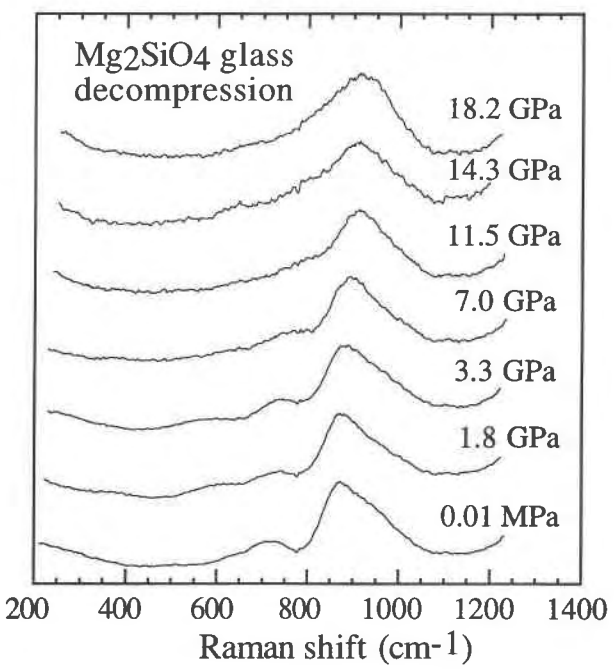

Fig. 7. In situ Raman spectra of forsterite glass under decompression. Scattering intensity on the low-frequency side of the main Raman band is lost below ~12 GPa.

loss in intensity is real or due to a shift of this weak band into the broadened manifold of the main Raman band. No other major changes in the spectrum are evident up to 20 GPa, and all frequency shifts are fully reversible over this pressure range.

As in the crystal, significant changes become evident in the Raman spectra of forsterite glass at higher pressures. Above 20 GPa there is a gradual but marked increase in the breadth of the main Raman band, primarily arising from an increase in intensity between 700 and 900 cm^{-1} (Figs. 6 and 7). This broadening may result from the emergence of new Raman bands associated with structural features similar to those that appear in the crystal above 30 GPa. It also appears that the pressure derivative of the average frequency of the main Raman band decreases significantly above ~20 GPa. However, this is probably only a manifestation of the gradual build-up of intensity in the low-frequency shoulder of the main band.

The behavior of the vibrational modes of glass upon decompression (Fig. 7) is similar to that of the behavior displayed in the crystal. The general high-pressure spectral features are retained on decompression to ~12 GPa. Below this pressure there is a rapid loss of intensity between 700 and 900 cm^{-1}. On recovery of the sample at ambient conditions, the glass bands return to their initial positions, although the breadth of the main Raman band is somewhat greater than that of the uncompressed sample.

Because of the similarity between the ambient structures of crystalline and amorphous forsterite, it is reasonable that they would have similar compression mechanisms. We conclude that the Raman spectra are consistent with the interpretation that dimers form in forsterite glass above ~20 GPa and that the dimerization is reversible to 50 GPa. This dimerization may or may not be accompanied by a Si coordination increase. The lower pressure at which dimerization is inferred to begin for the glass may be a result of the increased orientational disorder between adjacent SiO_4 tetrahedra in the ambient glass, allowing a less constrained approach of the tetrahedra during compression.

Conclusions

Raman spectra of statically compressed forsterite suggest that a reversible formation of defect structures begins above ~30 GPa in the crystal and above ~20 GPa in the glass. The defects probably form through dimerization of adjacent SiO_4 tetrahedra, creating local features within the olivine architecture that are similar to β-phase Mg_2SiO_4. The formation of these defect structures is consistent with the theoretically predicted dynamic structural instability of olivine at high pressure (Guyot and Reynard, 1992). We suggest that the formation of dimer defects in metastable crystalline olivine is a prelude to the irreversible amorphization reported at higher pressures.

Acknowledgments

We thank F. Guyot for valuable discussions and Q. Williams and an anonymous reviewer for constructive reviews. This work has been funded

by the National Science Foundation under grants EAR-91-05510 and EAR-92-19504.

References cited

Besson, J.M., Pinceaux, J.P., and Anastopoulos, A. (1982) Raman spectra of olivine up to 65 kilobars. Journal of Geophysical Research, 87, 10773–10775.

Bouhifd, M.A., Guyot, F., Petit, P.E., and Richet, P. (1992) Pressure induced amorphization of olivine compounds (abs.). Eos, 73, 594.

Brown, J.M., Furnish, M.D., and McQueen, R.G. (1987) Thermodynamics for $(Mg,Fe)_2SiO_4$ from the Hugoniot. In M.H. Manghnani and Y. Syono, Eds., High pressure research in mineral physics, p. 373–384. American Geophysical Union, Washington, DC.

Chopelas, A. (1990) Thermal properties of forsterite at mantle pressures derived from vibrational spectroscopy. Physics and Chemistry of Minerals, 17, 149–156.

Cooney, T.F., and Sharma, S.K. (1990) Structure of glasses in the systems Mg_2SiO_4-Fe_2SiO_4, Mn_2SiO_4-Fe_2SiO_4, Mg_2SiO_4-$CaMgSiO_4$, and Mn_2SiO_4-$CaMnSiO_4$. Journal of Non-Crystalline Solids, 122, 10–32.

Durben, D.J., and Wolf, G.H. (1991) Raman spectroscopic study of the pressure-induced coordination change in GeO_2 glass. Physical Review, B43, 2355–2363.

Guyot, F., and Reynard, B. (1992) Pressure-induced structural modifications and amorphization in olivine compounds. Chemical Geology, 96, 411–420.

Hazen, R.M. (1976) Effects of temperature and pressure on the crystal structure of forsterite. American Mineralogist, 61, 1280–1293.

Heymann, D., and Cellucci, T.A. (1988) Raman spectra of shocked minerals. 1. Olivine. Meteoritics, 23, 353–357.

Hofmeister, A.M., Xu, J., Mao, H.-K., Bell, P.M., and Hoering, T.C. (1989) Thermodynamics of Fe-Mg olivines at mantle pressures: Mid- and far-infrared spectroscopy at high pressure. American Mineralogist, 74, 281–306.

Jeanloz, R., and Kruger, M. (1992) Amorphization, shock waves and structure (abs.). Eos, 73, 594.

Kudoh, Y., and Takéuchi, Y. (1985) The crystal structure of forsterite Mg_2SiO_4 under high pressure up to 149 kb. Zeitschrift für Kristallographie, 171, 291–302.

Mao, H.-K., Xu, J., and Bell, P.M. (1986) Calibration of the ruby pressure gauge to 800 kbar under quasi-hydrostatic conditions. Journal of Geophysical Research, 91, 4673–4676.

McMillan, P.F., and Akaogi, M. (1987) Raman spectra of β-Mg_2SiO_4 (modified spinel) and γ-Mg_2SiO_4 (spinel). American Mineralogist, 72, 361–364.

McMillan, P.F., Akaogi, M., Ohtani, E., Williams, Q., Nieman, R., and Sato, R. (1989) Cation disorder in garnets along the $Mg_3Al_2Si_3O_{12}$-$Mg_4Si_4O_{12}$ join: An infrared, Raman and NMR study. Physics and Chemistry of Minerals, 16, 428–435.

Piriou, B., and McMillan, P. (1983) The high-frequency vibrational spectra of vitreous and crystalline orthosilicates. American Mineralogist, 68, 426–443.

Rao, K.R., Chaplot, S.L., Choudhury, N., Ghose, S., Hastings, J.M., Corliss, L.M., and Price, D.L. (1988) Lattice dynamics and inelastic neutron scattering from forsterite, Mg_2SiO_4: Phonon dispersion relations, density of states and specific heat. Physics and Chemistry of Minerals, 16, 83–97.

Richard, G., and Richet, P. (1990) Room-temperature amorphization of fayalite and high-pressure properties of Fe_2SiO_4 liquid. Geophysical Research Letters, 17, 2093–2096.

Sung, C.M., and Burns, R.G. (1976) Kinetics of the olivine-spinel transition: Implications to deep-focus earthquakes genesis. Earth and Planetary Science Letters, 32, 165–170.

Syono, Y., and Goto, T. (1982) Behavior of single-crystal forsterite under dynamic compression. In S. Akimoto and M.H. Manghnani, Eds., High pressure research in geophysics, 12, p. 563–578. Center for Academic Publications, Tokyo.

Syono, Y., Goto, T., Takei, H., Tokanami, M., and Nobugai, K. (1981) Dissociation reaction in forsterite under shock compression. Science, 214, 177–179.

Wang, S.Y., Sharma, S.K., and Cooney, T.F. (1993) Micro-Raman and infrared spectral study of forsterite under high pressure. American Mineralogist, 78, 469–476.

Will, G., Hoffbauer, W., Hinze, E., and Lauterjung, J. (1986) The compressibility of forsterite up to 300 kbar measured with synchrotron radiation. Physica, 139/140B, 193–197.

Williams, Q., McMillan, P., and Cooney, T.F. (1989) Vibrational spectra of olivine composition glasses: The Mg-Mn join. Physics and Chemistry of Minerals, 16, 352–359.

Williams, Q., Knittle, E., Reichlin, R., Martin, S., and Jeanloz, R. (1990) Structural and electronic properties of Fe_2SiO_4-fayalite at ultrahigh pressures: Amorphization and gap closure. Journal of Geophysical Research, 95, 21549–21563.

Xu, J., Mao, H.K., Weng, K., and Bell, P.M. (1983) High-pressure, Fourier-transform infrared spectra of forsterite and fayalite. Carnegie Institution of Washington Year Book, 82, 350–352.

Manuscript received July 7, 1993
Manuscript accepted July 23, 1993